# [illegible]

[illegible]

[illegible]

[illegible]

## [illegible]

[illegible]

[illegible]

[illegible]

## [illegible]

[illegible]

[illegible]

[illegible]

[illegible]

[illegible]

[illegible]

[illegible]

[illegible]

placed at (-10, 46.7), (0, 48.7), and (10, 47.7) $mm$ inside a background media. The microwave source is excited at 3.6 $GHz$, and it has pulse width of 1 $\mu s$ and a power of 1000 $W$. During this time, the target, as well as the background material, is heated; and, therefore, the pressure wave is generated due to thermal expansion. Finally, the acoustic wave impinges on the surface of the holey cavity, which randomizes the fields collected by the receivers. The properties of the materials used in this simulation are listed in Table I, where $\rho$ is density in $kg/m^3$, $c$ is the speed of sound in $m/s$, $C_p$ is the heat capacity in $J/(kg \cdot K)$, $k$ is the thermal conductivity in $W/(m \cdot K)$, $\alpha$ is the coefficient of thermal expansion in $1/K$, $\epsilon$ is the relative permittivity, and $\sigma$ is the conductivity in $S/m$.

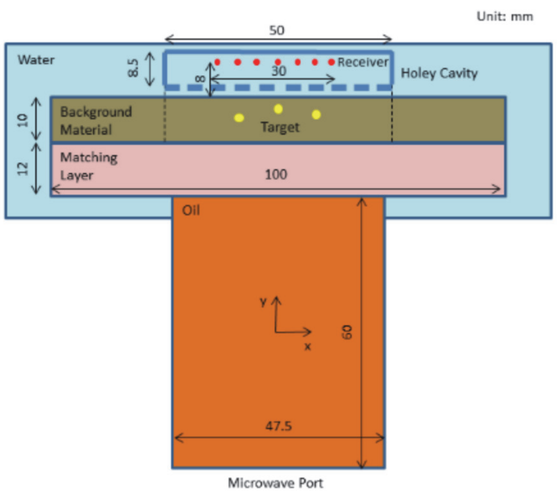


Fig. 1. A waveguide filled with oil is excited with a microwave source. The matching layer is put between the background material and the waveguide, to enhance the coupling of the microwave signal into the imaging region. The background material and the targets are surrounded by water. The cavity has 9 uniformly distributed openings, and it is set 2 mm above the background material. The receivers are placed inside the holey cavity.

TABLE I
MATERIAL PROPERTY

| Material | $\rho$ | $c$ | $C_p$ | $k$ | $\alpha$ | $\epsilon$ | $\sigma$ |
|---|---|---|---|---|---|---|---|
| Oil | - | - | - | - | - | 2.1 | 7e-5 |
| Matching Layer | - | - | - | - | - | 6 | 2e-3 |
| Background Material | 1020 | 1510 | 3550 | 0.21 | 3e-4 | 4.67 | 0.11 |
| Target | 1041 | 1580 | 3510 | 0.6 | 3e-4 | 53.9 | 2.45 |

of the ADMM imaging, shown in Fig. 3 (center), are more focused around the targets. Finally, when the holey cavity is used with the 3 receivers, the artifacts in both the Hermitan imaging and the ADMM imaging are further reduced, as shown in Fig. 3 (bottom), thus showing its effectiveness.

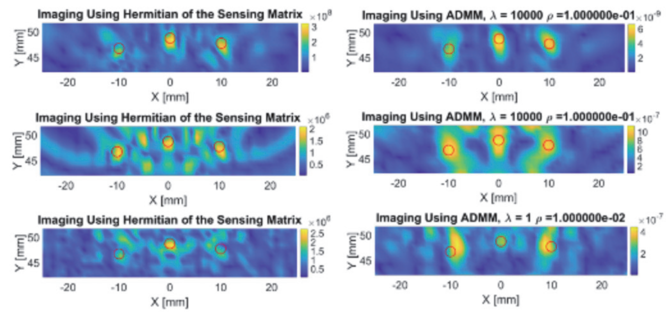


Fig. 2. Imaging results with different configurations. (Top) No cavity with 7 receivers for (left) the Hermitian method and (right) ADMM method. (Center) No cavity with 3 receivers for (left) the Hermitian method, and (right) ADMM method. (Bottom) Cavity with 3 receivers for (left) the Hermitian method, and (right) the ADMM method.

## IV. Conclusion

This work proposes the use of CS techniques for TA imaging when the acoustic receivers are located inside of a holey cavity. The proposed method and hardware architecture enables image reconstruction using a reduced number of measurements, which will reduce the complexity of data acquisition of the TA system. The optimization of the shape, size, and materials used to build the cavity will be addressed in future works.

## Acknowledgement

This work has been partially funded by the Department of Energy (Award No. DE-SC0017614) and the NSF CAREER program (Award No. 1653671).

## References

[1] X. Wang, D. R. Bauer, R. Witte, and H. Xin, "Microwave-induced thermoacoustic imaging model for potential breast cancer detection," *IEEE Transactions on Biomedical Engineering*, vol. 59, no. 10, pp. 2782–2791, 2012.

[2] Y. Cui, C. Yuan, and Z. Ji, "A review of microwave-induced thermoacoustic imaging: Excitation source, data acquisition system and biomedical applications," *Journal of Innovative Optical Health Sciences*, vol. 10, no. 04, p. 1730007, 2017.

[3] A. M. J. H. Ashkan Ghanbarzadeh Dagheyan, Chang Liu and J. M. Lorenzo, "Ultrasound imaging with compressive sensing via a holey